Chapter 11

Quantifying Strain-Sensing Protein Recruitment During Stress Fiber Repair

Shailaja Seetharaman, Stefano Sala, Margaret L. Gardel, and Patrick W. Oakes

Abstract

A family of proteins have been identified that recognize damaged, strained actin filaments in stress fibers. These proteins are often referred to as strain- or force-sensing and trigger downstream signaling mechanisms that can facilitate repair at these strain sites. Here we describe a method using high-resolution microscopy to screen and quantify the mechanosensitive recruitment of proteins to these stress fiber strain sites. Strain sites are induced using spatially controlled illumination of UV light to locally damage actin stress fibers. Recruitment of potential strain-sensing proteins can then either be compared to (Blanchoin, Physiol Rev 94, 235–263, 2014) a known control (e.g., zyxin-GFP) or (Hoffman, Mol Biol Cell 23, 1846–1859, 2012) the pre-damaged stress fiber protein distribution. With this method, strain-sensing proteins and their dynamic association with stress fiber strain sites can be reproducibly measured and compared.

Key words Stress fiber strain sites, Laser photoablation, LIM proteins, Zyxin, Testin, Stress fibers, Mechanosensing

1 Introduction

Actomyosin stress fibers (SFs) are load-bearing structures that form a major part of the mechanotransduction machinery in adherent cells, and are important for a wide range of cellular processes including cell migration, adhesion, and wound healing [1]. They are coupled to the cellular microenvironment via focal adhesions, enabling them to change their composition and assembly dynamics in response to extracellular cues. Increased SF tension can result in local SF damage and mechanical failure, which can either be induced experimentally or occur spontaneously in living cells. During the subsequent remodeling process, mechanosensitive proteins

---

Authors Shailaja Seetharaman and Stefano Sala have equally contributed to this chapter.
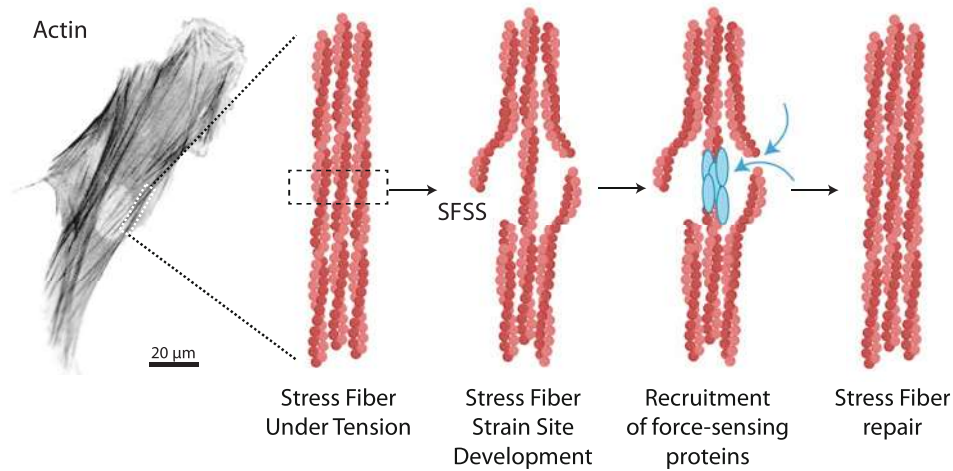
Fig. 1 Schematic of stress fiber strain site and repair. The development of a SFSS occurs either spontaneously in cells or can be induced by laser photoablation. This results in the rapid recruitment and accumulation of mechanosensitive proteins such as zyxin and testin to these SFSS. The damage sites are then repaired as zyxin recruits other proteins like VASP and α-actinin that promote actin assembly and cross-linking, respectively. (Created with BioRender.com)

such as some LIM domain proteins (e.g., zyxin, testin) localize to these stress fiber strain sites (SFSS) [2–7], and recruit actin polymerizing and crosslinking proteins, including VASP and α-actinin, to facilitate SF repair [8] (Fig. 1).

Several tools and methods have been developed to study the mechanical properties of SFs and the force-sensing mechanisms associated with SF damage and repair [9]. These include in vitro reconstitution of purified proteins and in vivo techniques such as traction force and atomic force microscopy, as well as whole-cell stretching and shearing. A powerful in vivo method to induce SF strain sites is laser photoablation. Here, we describe a method to induce SFSS by laser photoablation of individual SFs and quantify the recruitment of mechanosensitive proteins to these sites of strain [3, 5]. We describe cell culture and transfection protocols, followed by a detailed protocol for laser ablation, image acquisition, and analyses, primarily focusing on LIM domain proteins as representative mechanosensitive proteins that recognize SFSS. This method, however, can be utilized to visualize any protein of interest that might be important in SF strain-sensing or repair.

2   Materials

2.1   Cells and Culture Media

1. Zyxin$^{(-/-)}$ + EGFP-zyxin mouse embryonic fibroblasts (MEFs; cells were a gift of Mary Beckerle's laboratory, University of Utah, Salt Lake City, UT [2, 10]), or human foreskin fibroblasts (HFF) (*see* **Note 1**).

2. Fibroblast culture media: Dulbecco's Modified Eagle Medium (DMEM), 10% fetal bovine serum, 1% penicillin–streptomycin antibiotics, 1% antimycotic solution, 2 mM L-glutamine (*see* **Note 2**).

2.2 Constructs

Plasmid DNA encoding is a fluorescently tagged version of the protein(s) of interest (*see* **Note 3**). In this protocol we used the following constructs:

1. Zyxin-LCR-mCherry (LCR: LIM containing region)
2. Zyxin-FL-mCherry
3. NES-mCherry
4. GFP-Testin-FL
5. GFP-LIM 1-2-3 (the LIM domains from Testin)
6. mApple-actin

2.3 Transfection Equipment

1. TrypLE Express
2. 60 mm tissue culture dish
3. 22 × 30 mm glass coverslips
4. Neon™ transfection system (Invitrogen)
5. Neon™ transfection reagents: Resuspension Buffer R (MPK10096R) and Electrolytic Buffer E2 (MPK10096E)
6. Neon™ pipette (MPP100)
7. Neon™ tubes (MPT5)
8. Neon™ disposable tips, 100 μL (MPK10096T)
9. Cell counter

2.4 Microscope

1. Spinning Disk Confocal Unit (*see* **Note 4**)
2. Laser Launch with appropriate lasers for exciting green and red fluorophores
3. sCMOS camera
4. Spatial light modulation unit (*see* **Note 5**)

3 Methods

3.1 Transfections (see Note 6)

1. Place a sterile 22 × 30 mm coverslip into a fresh 60 mm tissue culture dish. Add 5 mL cell culture media and put the dish in the incubator at 37 °C (*see* **Note 7**).
2. Transfer 3 mL Electrolytic Buffer E2 into a Neon™ tube and place the Neon™ tube into the Neon™ pipette station.
3. Mix 110 μL Resuspension Buffer R with 1–5 μg DNA of choice. For example, we often used 2.5 μg plasmid DNA

encoding fluorescently tagged actin mixed with 2.5 μg plasmid DNA encoding, a fluorescently tagged version of the LIM protein of interest (*see* **Note 6**).

4. Detach the cells by adding 0.5 mL of TrypLE Express to an 80–90% confluent 60 mm dish. Incubate at 37 °C for 3–5 min until all the cells are completely detached (*see* **Note 8**).

5. Count the cells.

6. Transfer the appropriate volume containing 500,000 cells into a 15 mL conical and centrifuge for 3 min at 1500 rpm (*see* **Note 9**).

7. Aspirate the cell media and resuspend the cell pellet in the solution containing Resuspension Buffer R and DNA. Transfer the mixture to a 1.5 mL Eppendorf tube (*see* **Note 10**).

8. Insert a Neon™ disposable tip into the Neon® pipette.

9. Carefully aspirate the cell and DNA solution (1.5 mL Eppendorf tube) with the Neon™ tip and insert the Neon™ pipette into the Neon™ tube in the Neon™ pipette station (*see* **Note 11**).

10. Select the appropriate electroporation protocol. For fibroblasts we used 1 pulse of 1600 V applied to the cells (*see* **Note 12**).

11. Unplug the Neon™ pipette as soon as the electroporation is done and transfer the cells into the 60 mm dish containing 22 × 30 mm coverslip.

12. Place the cells in the incubator and wait 24 h before imaging to ensure sufficient protein expression (*see* **Note 13**).

3.2 Image Acquisition

1. Live cell imaging and laser photoablations are performed using confocal spinning disk microscopes that contain 405, 491, 561, and 642 nm laser lines, an sCMOS camera, motorized X, Y stage, and a spatial light modulation unit. For exact system details, *see* **Note 4**. During image acquisition, keep imaging settings constant between different cells and samples (*see* **Note 14**).

2. Transfer the imaging chamber into the microscope incubator and let the sample equilibrate for at least 5 min to avoid thermal fluctuations and hence drifting during imaging.

3. Acquire several images of the cell culture media region without cells in each channel before an imaging experiment. This will act as the background signal from camera noise, media fluorescence, etc.

4. Select cells that express the constructs of interest (in this case, the mCherry-zyxin-FL or GFP-Testin), mApple-actin, and/or GFP-zyxin using a high magnification (e.g., 60X or 63X) objective.

5. Select a SF to induce strain in, and draw a small area targeting a region of interest on the SF. A 5-μm ablation line perpendicular to the orientation of the fiber is used to induce a SFSS as depicted in Fig. 3 (*see* **Note 15**).

6. Image the "steady state" by acquiring 30 s–1 min pre-ablation, alternating between both channels (*see* **Note 16**).

7. Illuminate the ablation line with a 405 nm laser for ~1.5 s at a power density of ~350 μW/μm^2 to induce a stress fiber strain site (*see* **Note 17**).

8. Continue the timelapse for the desired duration (e.g., Supplemental Movie 1 is 3 min and 30 s; *see* **Note 18**), imaging both channels at a consistent time interval ranging from 2 to 20 s.

9. Save the ablation region for analysis.

10. Export all images (containing both the actin and LIM protein channels) as 16-bit TIFF files.

3.3 Image Analysis

Two different analyses methods to observe recruitment of proteins to SFSS are described below. In the first case, cells expressing measurements of protein recruitment (mCherry-tagged) are made in cells stably expressing GFP-zyxin. In the second case, cells do not stably express any protein, and the enrichment of the protein of interest (GFP-tagged) is measured with respect to the signal prior to the ablation. Ultimately, both analyses methods yield measurements of the recruitment of LIM proteins to the strain sites on SFs.

Intensity Relative to GFP-Zyxin The following steps will calculate the ratio of the mean fluorescence intensity of the transiently transfected mCherry tagged protein of interest to the fluorescence of the stably integrated GFP-zyxin. This provides a measurement of the enrichment of the protein of interest at the SFSS (Fig. 2).

1. *Open image files as a sequence/movie on ImageJ and identify the region of ablation in each channel.*

2. *Using the ImageJ reslice function, draw kymographs in the region of ablation in each channel (see **Notes 19 and 20**).*

3. *Generate a line profile by drawing a line scan (shown in red, Fig. 2a, d, h) across the kymograph (through the time axis).*

4. *Plot the raw line scans as shown in Fig. 2b, e, h.*

5. *Consider the background as the region on the fiber where the future strain sites develop. Calculate intensity of the signal immediately before the SFSS is formed. Subtract this signal from both channels (mCherry-background and GFP-zyxin-background).*

6. *The background subtracted line scans are plotted in Fig. 2c, f, i.*

7. *To obtain the enrichment for each channel, determine the peak of the curves (shown as dotted circles; Fig. 2c, f, i) to get the*
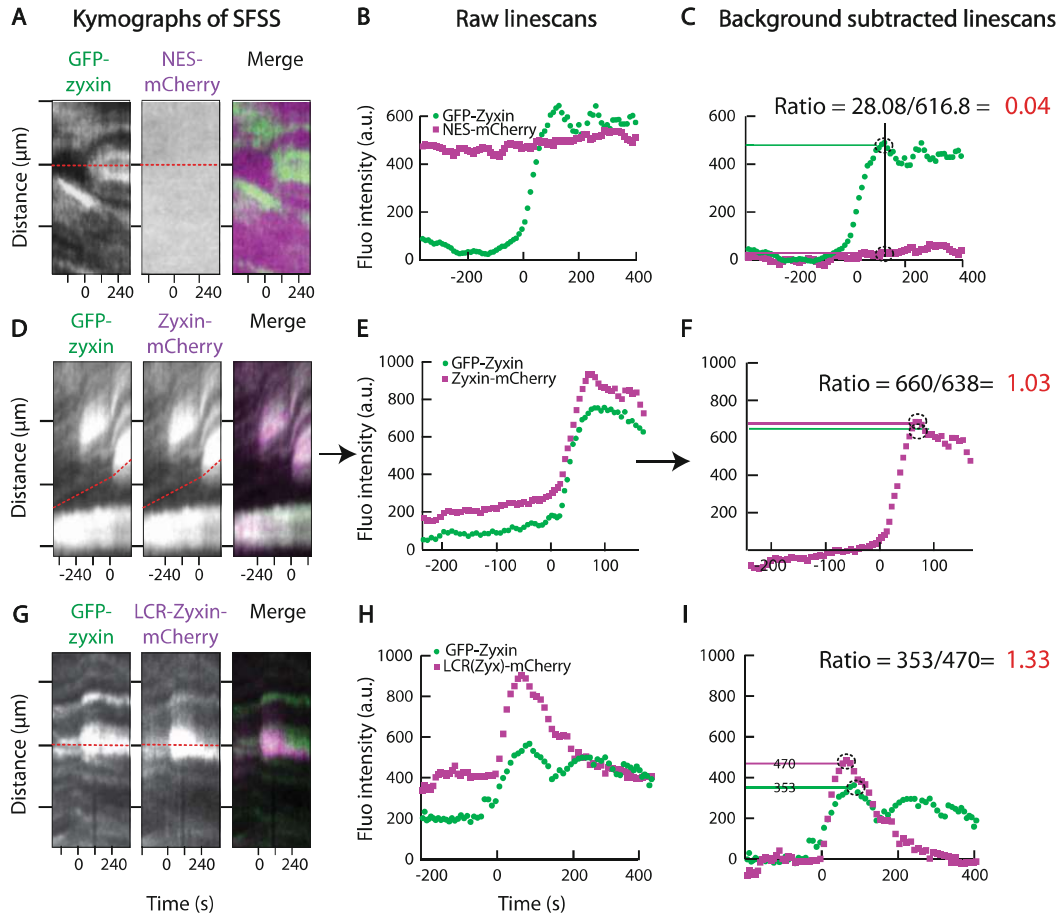
Fig. 2 Quantification of relative LIM protein recruitment to laser photoablation-induced stress fiber strain sites. (**a**, **d**, **g**) Kymographs from movies of GFP-zyxin-integrated fibroblasts that are transfected with an mCherry-construct of interest (in this case, a construct of nuclear export signal NES-mCherry (**a**) used as negative control, zyxin-mCherry as positive control (**d**), and LCR-zyxin-mCherry as the construct of interest (**g**) are transiently transfected). (**b**, **e**, **h**) Raw line scans through kymographs (marked in red) shown in (a), (d), and (g). (**c**, **f**, **i**) Background subtracted line scans where the signal before the development of a SFSS is subtracted. The peak of each curve (shown as dotted circles) is determined and averaged across two adjacent data points. This provides the enrichment of the construct at the site. This enrichment is then divided by the enrichment of GFP-zyxin to calculate the main mCherry:GFP fluorescence ratio (depicted in red) as described in the Image Analysis Subheading 3.3. Scale bar: 2 μm. (Figure adapted from Winkelman et al., 2020)

maximum fluorescence intensity, and average this with the two adjacent points (see **Note 21**; denoted as mCherry-construct-SFSS or GFP-zyxin-SFSS).

8. Divide the enrichment of mCherry-construct by the enrichment of GFP-zyxin to obtain the main metric fluorescence ratio as follows:

$$\text{mCherry : GFP ratio} = \left(\frac{(\text{mCherry} - \text{construct} - \text{SFSS}) - (\text{mCherry} - \text{background})}{(\text{GFP} - \text{zyxin} - \text{SFSS}) - (\text{GFP} - \text{zyxin} - \text{background})} \right.$$

Intensity Relative to Pre-ablation For the enrichment of a GFP-tagged, LIM protein of interest being recruited to SFSS in fibroblasts. Simultaneous monitoring of mApple-actin signal in the region of the SFSS can confirm that the SF is damaged during ablation and that repair is occurring over the timelapse. All movies are analyzed in Python as outlined below and described in Sala et al., 2021, and Fig. 3. The code, along with example data, is available at https://github.com/OakesLab/Sala_MBoC_2021.

1. *Break down each movie into the individual stacks representing the actin and LIM protein channels.*

2. *For each stack, perform a flat field and dark field correction. Flat field corrections are performed by dividing the image by a normalized image of uniform intensity. Dark field corrections are done by subtracting an image of the camera taken without opening the shutter* (see **Note 22**).

3. *Correct each stack for photobleaching by fitting the intensity sum of each frame to an exponential decay of the form* $I = A\,e^{-B * t}$, *where* A *and* B *are fit parameters. To create a correction curve, we divide the value at* $t = 0$ *by the values at all other time points. Correct each frame by multiplying the intensities in each frame by the corrected value at that time point* (see **Note 23**).

4. *Register the corrected image stack of the LIM protein to the first frame by calculating the registration shifts using any registration routine* (see **Note 24**).

5. *Register the actin channel based on the calculated shifts of the channel representing the LIM protein.*

6. *Crop both registered stacks to a region of 121 × 121 pixels (approximately 21 × 21 μm) centered on the midpoint of the ablation line (Fig. 3).*

7. *For the cropped LIM protein stack, create a circular "ablation mask" with a radius of 20 pixels around the midpoint of the ablation line (Fig. 3).*

8. *Expand the ablation mask three times (radius of 60 pixels) to create a "ROI mask" (Fig. 3).*

9. *Make a mask of the entire cell. Multiply both the ablation mask and ROI mask by the cell mask to ensure that all downstream calculations are done only on pixels that are inside the cell.*

10. *Create a reference intensity image (I_{ref}) for both the actin and LIM protein stacks by calculating the average intensity of each pixel from the frames before the photoablation in each channel.*

11. *For every frame in both channels, subtract the reference image (I_{ref}) from the given frame (I_t) and divide by the reference image. This will create a relative difference intensity image ($I_{diff} = (I_t - I_{ref})/I_{ref}$) for each time point* (see **Note 25**).
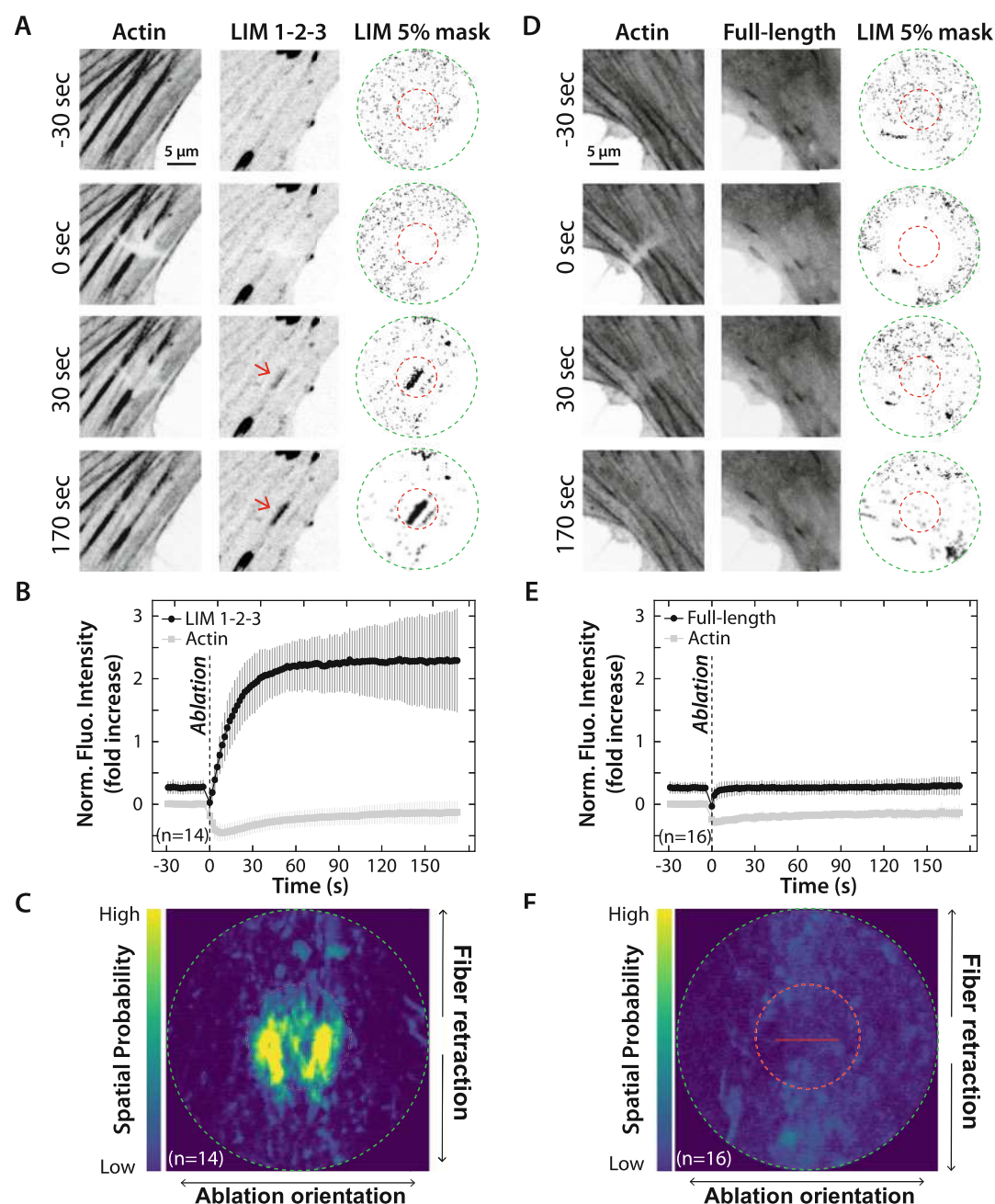
Fig. 3 Quantification of LIM protein recruitment to photoablation-induced stress fiber strain sites. (**a**, **d**) HFFs co-expressing mApple-actin and GFP-coupled versions of either a mechanosensitive LIM construct (LIM domains of testin (LIM 1-2-3) (**a**), or a non-mechanosensitive LIM construct (full-length testin (**d**). The images show the localization of the actin and LIM constructs during a laser photoablation experiment ("0 sec" indicates the photoablation timepoint, *see* Supplemental Movie S1). The LIM 5% masks show the pixels in the ROI (green dashed circle) that changed the most in intensity in the LIM channel compared to their pre-ablation state. The red arrows indicate relocation of the mechanosensitive LIM domains of testin to laser-induced stress fiber strain sites as the brightest pixels in the LIM 5% mask are located inside the ablation region (red

12. *Make a mask of the 5% brightest pixels in the LIM protein channel (LIM 5% mask) for both the ROI mask and ablation mask zones (Fig. 3a, d).*

13. *For both the LIM and actin channels, calculate the average intensity value of the pixels that match the position of the 5% brightest pixels in the ablation region (red dashed circle in Fig. 3a, d) of the LIM 5% mask. Plot these average values over time for both channels to create a trace of the normalized fluorescence intensities (see **Note 26**).*

14. ***Steps 1–13*** *should be repeated for every movie that is made. Based on the total number of movies, an average fluorescence intensity trace (**step 15**) and spatial probability map of recruitment (**step 16**) can be created.*

15. *To create an average trace of all analyzed movies, calculate and plot the averaged normalized fluorescence intensity value ± standard deviation of each time point for both the actin and LIM protein channels (Fig. 3b, e).*

16. *To create a spatial probability map of the LIM protein, sum all the LIM 5% masks across the entire stack for each movie (summed LIM mask). Rotate the resulting summed LIM masks so that the direction of the ablation is aligned horizontally and average them across all movies (Fig. 3c, f).*

4   Notes

1. Cells should be cultured at 37 °C with 5% CO_2 and passaged when a confluency of 80–90% is reached.

2. Imaging media can be used during acquisition: Leibovitz's L-15 medium without phenol red, 10% fetal bovine serum, 1% antibiotic, antimycotic solution.

Fig. 3 (continued) dashed circle). This relocation is not observed for the non-mechanosensitive full-length testin construct as confirmed by a random distribution of the pixels in the LIM 5% mask. (**b**, **e**) Average fluorescence traces and standard deviations of the actin intensity and intensities of either LIM 1-2-3 of testin (**b**) or full-length testin (**e**) based on a total of *n* photoablation experiments. Following the induction of a stress fiber strain site, a rapid increase of the LIM 1-2-3 signal occurs, which coincides with a loss of the actin signal as it is damaged (**b**). The LIM signal plateaus as the damaged actin gets repaired (**b**). This increase is not observed for the full-length construct, indicating it is not recruited to stress fiber strain sites (**e**). (**c**, **f**) Spatial probability recruitment maps of the LIM domains of testin (**c**) and full-length protein (**f**) based on a total of *n* photoablation experiments. The brightest LIM 1-2-3 pixels are located in the ablation region (red dashed circle), which is indicative of strain recognition. The brightest pixels of the full-length construct are distributed randomly within the ROI (green dashed circle). The red line represents the 5-μm ablation line. (Figure adapted from Sala et al., 2021)

3. In the experiments shown here, cells are transiently transfected with fluorescently tagged constructs. As protein overexpression often disrupts their natural stoichiometry and causes off target effects (e.g., mis-localization, pathway (in)activation [11]), the creation of a stable cell line using a lentiviral expression system or CRISPR technology might be beneficial to obtain similar protein expression levels and minimize heterogeneity. In addition to the type of fluorescent protein used for tagging, it is important to consider where to add the fluorescent tag. The tag can be fused either at the N- or C-terminal, depending on the structure and folding of the protein of interest, and its subsequent localization within the cell. Note that the functionality and localization of some proteins can be maintained only if the tag is placed on the appropriate terminus. Finally, the protocol described in this chapter involves time-lapse imaging. To prevent photobleaching, it is recommended that a fluorophore with high photostability, such as EGFP or mEmerald, be used for tagging.

4. The exact makeup of the microscope for these experiments is flexible. The following microscopes and setups were used for image acquisition:

   (A) Inverted Nikon Ti-E microscope (Nikon, Melville, NY) with a Yokogawa CSU-X confocal scanhead (Yokogawa Electric, Tokyo, Japan) and laser merge module containing 491, 561, and 642 nm laser lines (Spectral Applied Research, Ontario, Canada). Images were collected on Zyla 4.2 sCMOS Camera (Andor, Belfast, UK). A 405 nm laser coupled to a Mosaic digital micromirror device (Andor) was used to locally damage SF. Images were collected using a 60X 1.49 NA Apo-TIRF oil immersion objective (Nikon). All hardware was controlled using MetaMorph Automation and Image Analysis Software (Molecular Devices, Sunnyvale, CA). (B) Marianas Imaging System (Intelligent Imaging Innovations) consisting of an Axio Observer 7 inverted microscope (Zeiss) attached to a W1 Confocal Spinning Disk (Yokogawa) with Mesa field flattening (Intelligent Imaging Innovations), a Phasor photo-manipulation unit (Intelligent Imaging Innovations), a motorized X, Y stage (ASI), and a Prime 95B sCMOS (Photometrics) camera. Illumination is provided by a TTL triggered multifiber laser launch (Intelligent Imaging Innovations) consisting of 405, 488, 561, and 637 lasers, using a 63 × 1.4 NA Plan-Apochromat objective (Zeiss). Temperature and humidity are maintained using a Bold Line full enclosure incubator (Oko Labs). The microscope is controlled using Slidebook 6 Software (Intelligent Imaging Innovations).

5. Like microscopes, the spatial light illumination module is flexible, as long as sufficient power can be concentrated in small region. For these experiments an Mosaic digital multimirror (DMM) device (Andor) or a Phasor holographic photomanipulation unit (Intelligent Imaging Innovations) were used.

6. For transient transfection, electroporations are preferred since they usually yield high transfection efficiencies and protein expression levels. For certain cell types, however, a low viability is observed post electroporation in which case we recommend using other transfection methods and optimizing transfection conditions to improve cell survival. The quantity of transfected DNA can vary. High concentrations of transfected DNA can lead to low cell viability post electroporation. In the experiments described in Fig. 2, cells expressing high levels of transfected zyxin display an increased accumulation of zyxin at SFSS, and is inversely correlated with paxillin recruitment to the SFSS (*see* Fig. 2G-I and S2A in Winkelman et al., 2020 [3]). Thus, it is important to note that high expression levels of proteins can lead to competition in force-sensing.

7. Any size coverslip and imaging chamber can be used. For laser photoablation experiments, however, cells should be plated as single cells following transfection. We therefore recommend using a coverslip and tissue culture dish size that match these requirements (*see* **Note 9**).

8. Limit the time that the cells are in the TrypLE Express solution to increase cell viability. Gently tapping the tissue culture dish can speed up their detachment.

9. The number of cells chosen for transfection should match the optimal plating density for imaging (*see* **Note 7**).

10. Avoid creating air bubbles when the cells are resuspended in Resuspension Buffer R as it can cause arcing during electroporation which results in increased cell death.

11. Avoid creating air bubbles when the cells and DNA are aspirated with the Neon™ tip (*see* **Note 10**).

12. Voltage and number of pulses are cell type-dependent and crucial for optimal cell viability and transfection efficiency. We refer to the *cell line data and transfection parameters* listed on the manufacturer's website (www.thermofisher.com).

13. If a significant amount of cell death is observed 2–3 h post transfection, the cell media should be changed.

14. Although this method can be used to locally induce SFSS in cell monolayers, the experiments depicted here were carried out in single cells. Parameters such as cell density and cell–cell contacts must be taken into consideration and kept similar across the various samples. In addition, cells with abnormal nuclei,

blebbing, retraction, or experiencing phototoxic effects must be excluded during data acquisition and analysis. We found that using ~2.5 mW of power (measured at the objective) is sufficient to produce high signal-to-noise intensity measurements with minimal phototoxic effects with both our 488 and 561 nm lasers.

15. It is very important to draw the ablation line perpendicular to the orientation of the stress fiber to ensure that all the individual actin filament that build up the selected fiber are illuminated. In this way, a subset of the actin filaments will be stochastically damaged, which causes the remaining undamaged fibers to be stretched under the increased load. Successful strain induction is obtained when recoil and thinning of the ablated stress fiber are observed.

16. The successful induction of a stress fiber strain site strongly depends on the illumination duration and intensity. If the illumination intensity is too low and/or the duration too short, insufficient damaged is caused to the stress fiber and hence no strain will be induced (no recoil or thinning are observed – though photobleaching will likely still occur). In contrast, if the illumination intensity is too high and/or the duration too long, actin filaments can be fully severed, resulting in a severed stress fiber that is no longer under tension. We therefore recommend optimizing the illumination intensity and duration when performing laser photoablations on a different sample.

17. A few frames (at least 10–15 images) should be acquired before the ablation event as these pre-ablation frames are used to create a reference intensity image to quantify potential LIM protein recruitment to stress fiber strain sites.

18. The representative movie is acquired for a total duration of 3 min and 30 s. In this case, the duration is precisely chosen because on the one hand, it allows enough time for the damaged actin to be repaired and for the LIM proteins that are recruited to these damaged actin sites to reach a plateau (*see* Fig. 3). On the other hand, it limits the amount of time the cells are exposed to light-reducing phototoxic effects. However, depending on the nature and purpose of the experiment, the duration of the movie can vary.

19. If cells or the stage moved significantly, align stacks before analysis. If SFs move significantly, use a python script in ImageJ to build kymographs from user-drawn line segments (as in [3]).

20. Always draw kymographs of the same length and angle with respect to the SF orientation.

21. If there was no obvious signal for the construct of interest being tested, then the time point at which GFP-zyxin signal was maximal was used in measuring the mCherry-construct signal.

22. To create flat fields, 30–50 fields of a soluble dye solution are taken (e.g., 100 mg/mL of FITC or Rose Bengal for green and red dyes). A flat field can then be calculated by taking the median of the stack of images (the median is preferred to the mean to avoid aggregates in any given image). The darkfield image is then subtracted from the median image, and the subsequent product is normalized by dividing by the maximum value. To correct an image, the darkfield image is first subtracted, and then the result is divided by the flat field image.

23. We often observe a two-step photobleaching response with mApple and mCherry constructs. This can be seen as a sudden dip in fluorescence intensity within the first few frames of a time-lapse experiment, followed by a slower and steadier photobleaching response. To avoid artifacts from this initial rapid photobleaching, we recommend disregarding the first 5 frames (i.e., the first few seconds of the steady state imaging, well before the ablation event) of each movie for analysis.

24. There are several plug-ins in FIJI that can accomplish image registration. We used a sub-pixel registration developed by Guizar-Sicairos et al [12]. This implementation can be downloaded in our GitHub repository (https://github.com/OakesLab/Sala_MBoC_2021).

25. The creation of a relative difference image allows the quantification of the highest intensity pixels due to enrichment (stress fiber strain site recruitment) of a LIM protein compared to its localization in the pre-ablation state. This avoids the detection of the brightest pixels before photoablation that do not change in intensity after the photoablation and thus avoids including LIM protein intensities in cellular compartments such as focal adhesions or the nucleus.

26. Inspection of the signal in the actin channel can provide insight into whether proteins are being recruited to an actual strain site. A damaged fiber should show a decrease in intensity in the actin channel that then increases over time, indicating that repair is taking place. If the actin channel instead increases concomitant with the LIM protein, it can suggest that the protein is simply recognizing all actin filaments and not strained filaments in particular. Repair is completed when actin intensity in these regions returns to its baseline value prior to ablation.

Acknowledgments

References

1. Blanchoin L, Boujemaa-Paterski R, Sykes C, Plastino J (2014) Actin dynamics, architecture, and mechanics in cell motility. Physiol Rev 94:235–263

2. Hoffman LM, Jensen CC, Chaturvedi A, Yoshigi M, Beckerle MC (2012) Stretch-induced actin remodeling requires targeting of zyxin to stress fibers and recruitment of actin regulators. Mol Biol Cell 23:1846–1859

3. Winkelman JD, Anderson CA, Suarez C, Kovar DR, Gardel ML (2020) Evolutionarily diverse LIM domain-containing proteins bind stressed actin filaments through a conserved mechanism. Proc Natl Acad Sci 117:25532

4. Oakes PW et al (2017) Optogenetic control of RhoA reveals zyxin-mediated elasticity of stress fibres. Nat Commun 8

5. Sala S, Oakes PW (2021) Stress fiber strain recognition by the LIM protein testin is cryptic and mediated by RhoA. Mol Biol Cell 32:1758–1771

6. Yoshigi M, Hoffman LM, Jensen CC, Yost HJ, Beckerle MC (2005) Mechanical force mobilizes zyxin from focal adhesions to actin filaments and regulates cytoskeletal reinforcement. J Cell Biol 171:209–215

7. Sun X et al (2020) Mechanosensing through direct binding of tensed F-actin by LIM domains. Dev. Cell 55:468–482.e7

8. Smith MA et al (2010) A zyxin-mediated mechanism for actin stress fiber maintenance and repair. Dev Cell 19:365–376

9. Kassianidou E, Kumar S (2015) A biomechanical perspective on stress fiber structure and function. Biochim Biophys Acta 1853:3065–3074

10. Hoffman LM et al (2003) Targeted disruption of the murine zyxin gene. Mol Cell Biol 23:70–79

11. Schwinn MK, Steffen LS, Zimmerman K, Wood KV, Machleidt T (2020) A simple and scalable strategy for analysis of endogenous protein dynamics. Sci Rep 10:8953

12. Guizar-Sicairos M, Thurman ST, Fienup JR (2008) Efficient subpixel image registration algorithms. Opt Lett 33:156–158